Nickel oxalate nanostructures for supercapacitors†

Insoo Jung, Jinsub Choi* and Yongsug Tak*

Received 3rd February 2010, Accepted 6th May 2010
DOI: 10.1039/c0jm00279h

Herein, we describe a facile method to produce nickel oxalate nanostructures by chemical reaction of oxalic acid and a nickel foil in various organic solvents and water. Grass-like structures consisting of nickel oxalate are produced by the chemical reaction within 30 min for all solvents. Interestingly, nickel oxalate nanowires can be produced by the addition of a small amount of water in certain solvents. Annealing of nickel oxalate structures leads to formation of nickel oxide structures with a slight morphological change. Compositions of the nanostructures are investigated by TEM and FT-IR analyses. In addition, the supercapacitance of the nickel oxalate nanostructures is characterized, and the results show that they are superior to that of nickel oxide nanostructures.

1. Introduction

Electrochemical capacitors (EC), so-called ultracapacitors or supercapacitors, have attracted considerable interest, since they have high power density with an order of magnitude higher than electrolytic capacitors and longer cycle life than rechargeable batteries.[1,2,3] They rely on either a capacitive or pseudocapacitive mechanism: the capacitive mechanism is attributed to non-faradaic double layer capacitance on the interface between an electrode and electrolyte and the pseudocapacitive mechanism is ascribed to faradaic charge transfer through redox reactions on the electrode.[1]

Many metal oxides, such as RuO_2, CoO_x, MnO_2, NiO, $Ni(OH)_2$, and so on, have been studied for EC applications.[4,5,6,7,8,9] Compared to hydrous RuO_2, which offers outstanding EC properties,[10,11] nickel oxide has benefits with respect to cost and material availability.[12,13] In addition, nickel oxide possesses good EC properties for both nonfaradaic and faradaic reactions. For a 3-D nickel oxide structure, specific capacitance with 3152 F g^{-1} was reported, exceeding that of ruthenium oxide (863 F g^{-1}). Recent studies have shown that nanostructured metal oxides are considered to be more suitable electrodes for EC, since they provide high specific surface area and fast redox reactions. In this report, we describe a new EC electrode consisting of nickel oxalate that can be prepared by a facile and cost effective process.

2. Results and discussion

Fig. 1 shows the morphological changes of nanostructures on Ni that are prepared in different solvents containing 1 M oxalic acid. All structures appear to have a similar morphology except for their size and density. The structure prepared in water resembles fused nanowires or nanowires that are not fully developed from a sheet (Fig. 1(a)), whereas large structures consisting of bundles of sheets are obtained when the aqueous solution is substituted by methanol (Fig. 1(b)). Similar to Fig. 1(a), grass-like structures are observed in the case of structures prepared in ethanol, *n*-propanol and *n*-butanol, respectively (Fig. 1 (c), (d) and (e)). Interestingly, as solvents with higher numbers of carbon chains are used, the density of nanostructures increases and the areas within the dotted lines in Fig. 1 decreases (see Table S1, ESI†). We suppose that seeds of the nanostructures in the demarcated areas do not exist. This strongly suggests that reaction in *n*-butanol provides the most seeding sites for formation of the nanostructures.

As a small amount of water is added into the solution, the morphologies of the nanostructures are greatly changed except for in the case where methanol is employed (see Fig. 2(a)). Ethanol, *n*-propanol and *n*-butanol lead to the formation of nanowires, as shown in Fig. 2(b), (c) and (d). Analogous to the results shown in Fig. 1, the density of the nanowires increases and their size decreases when solutions containing longer carbon chains are used.

The effects of water content on morphological changes of the nanostructures are presented in Fig. 3, showing that the diameter of the nanowires clearly increases as the water content increases. As shown in Fig. S1 (ESI†), pH values are not greatly changed as the water is added. Since a high concentration of oxalic acid is used, the pH value is less than 1 regardless of the amount of added water. This is due to increases in the concentrations of H^+ and OH^- when water is added. However, the absolute amount of H^+ and OH^- increases when water is added, greatly influencing the morphology of the nanostructures.

Nickel is dissolved in oxalic acid, resulting in the production of free nickel ions in the solution. The ions likely react with oxalic acid, creating a nickel oxalate complex based on a self-complex formation mechanism[14] and nickel can be better dissolved when the concentration of H^+ and OH^- ions is increased. Thus, the Ni source for making nanowires becomes more abundant when water is added. This allows for the fabrication of nanowires with a large diameter upon increased water content. As described in

Department of Chemical Engineering, Inha University, Incheon, 402-751, Korea. E-mail: jinsub@inha.ac.kr; ystak@inha.ac.kr; Fax: +82-32-866-0587; Tel: +82-32-860-7476/82-32-860-7471

† Electronic supplementary information (ESI) available: Table S1: The mean areas of non-seeded regions denoted in Fig. 1. Fig. S1: Variation of pH associated with the addition of amounts of water to ethanolic 1 M oxalic acid. Fig. S2: Initial growth of nanowires prepared in ethanolic 1 M oxalic acid without water addition. Fig. S3: Enlarged view of Fig. 7, showing peaks in the range of 400–1000 cm^{-1}. Fig. S4: Enlarged views of Fig. 8, showing double layer capacitance. See DOI: 10.1039/c0jm00279h

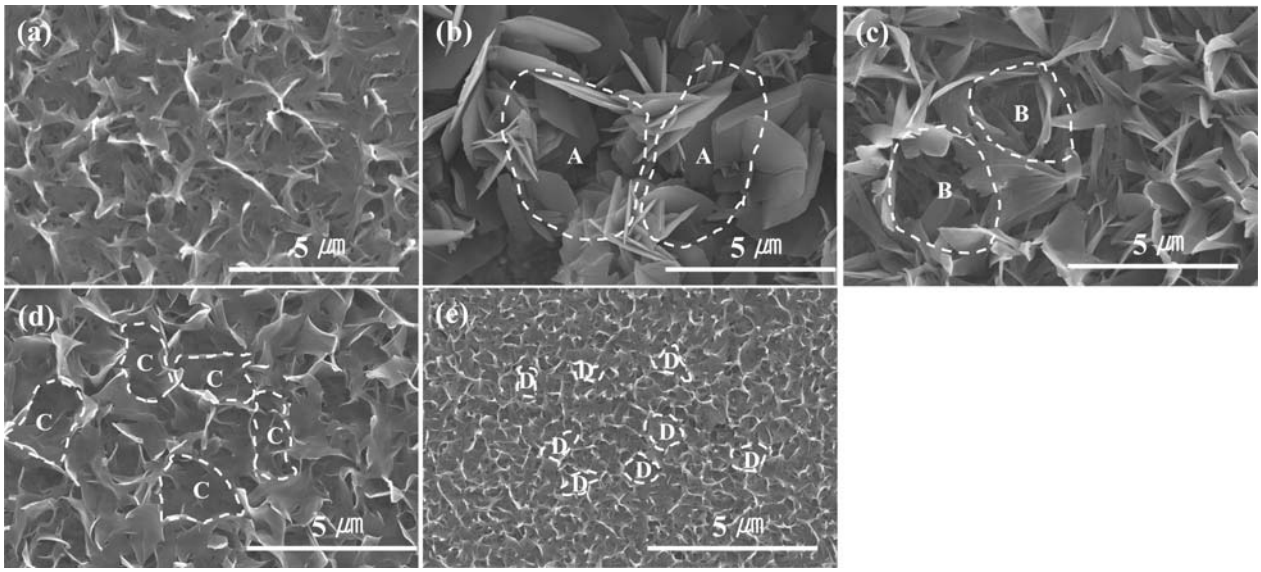

Fig. 1 FE-SEM images of the morphology of nickel oxalate nanostructures prepared in 1 M oxalic acid dissolved in different solvents: (a) deionized water, (b) methanol, (c) ethanol, (d) *n*-propanol, (e) *n*-butanol. All reactions are performed at 45 °C for 1.5 h. Note the areas within the dotted lines where no seeds for nickel oxalate structures are formed. The mean areas calculated by ImageProPlus software are tabulated in Table S1 (ESI†).

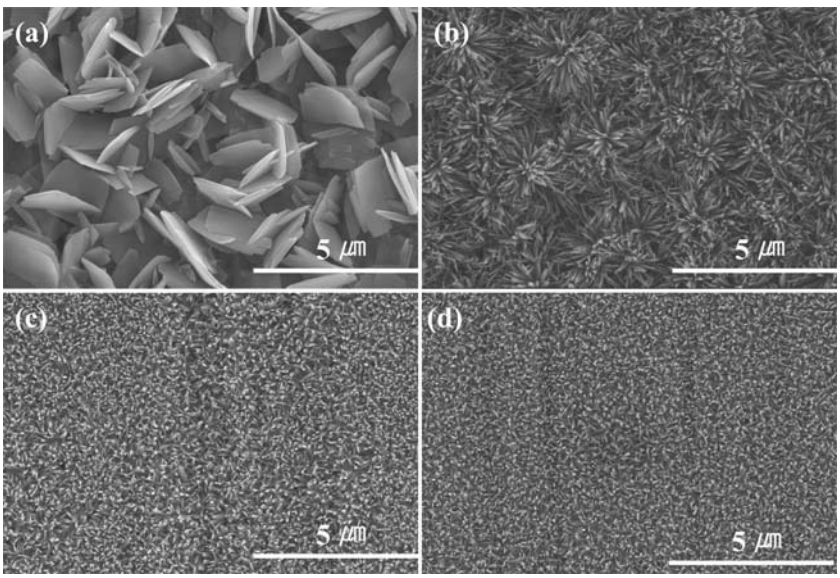

Fig. 2 Effect of the addition of 5% water to the different solvents on the morphological changes of nickel oxalate nanostructures. Reaction is carried out at 45 °C for 1.5 h in 1 M oxalic acid solutions of (a) methanol, (b) ethanol, (c) *n*-propanol and (d) *n*-butanol.

relation to Zn,[15] the nanowire formation mechanism appears to involve preferential precipitation of the nickel oxalate complex in organic solvents.

Initial growth of nanowires in ethanolic oxalic acid with 5 wt% water is clearly displayed in Fig. 4. Octahedral seeds with a size of less than 250 nm are observed in the case of 10 s reaction (Fig. 4(a)), and cubic morphologies with a size of less than 500 nm are prepared when the reaction is carried out for 1 min (Fig. 4(b)). Further reaction leads to the production of small cubic seeds with a size of less than 50 nm on the large cubic structures (Fig. 4(c)). The small cubic seeds can fully develop into cubic structures with a size of around 100 nm (Fig. 4(d)) if the reaction further proceeds. Finally, the structures become nanowires with a diameter of less than 50 nm within 5 min (Fig. 4(e)). This indicates that the roots of the structures consist of cubic structures with a size of 500 nm and nanowires with a diameter of less than 50 nm radially grow from these roots. For comparison, the morphological changes of samples prepared without water addition were studied as a function of reaction time (see Fig. S2, ESI†). Initial seed formation takes a longer time as compared to the results shown in Fig. 4, meaning that the reaction without water is slower. The density of grass-like structures increases and individual structures become more intricate as the reaction time increases. The surface of Ni is fully covered by these grass-like structures after roughly 30 min reaction.

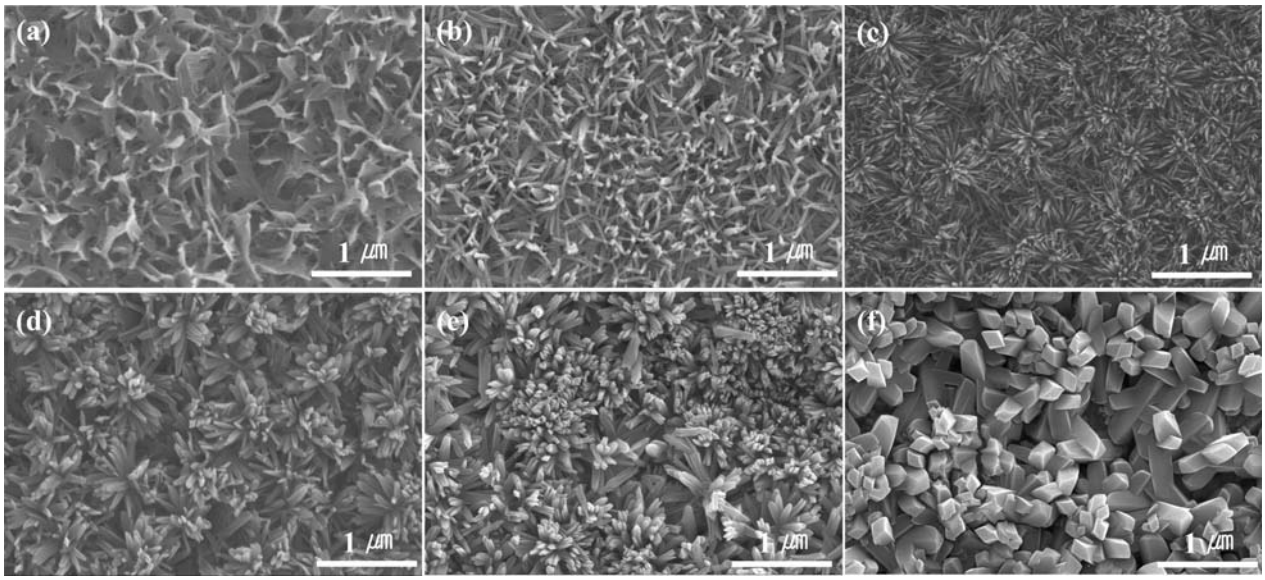

Fig. 3 Morphological changes of nanowires prepared in ethanolic 1 M oxalic acid according to the addition of water: (a) 1%, (b) 3%, (c) 5%, (d) 7%, (e) 40%, (f) 50%. Reaction is carried out at 45 °C for 1.5 h.

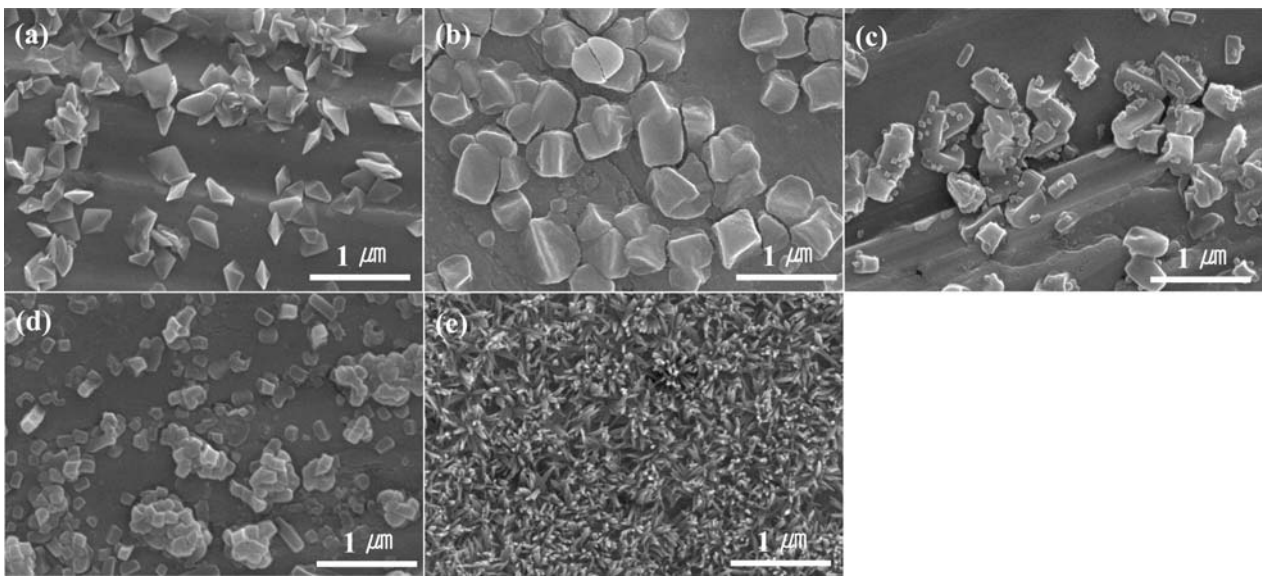

Fig. 4 Initial growth of nanowires prepared in ethanolic 1 M oxalic acid containing 5% water for (a) 10 s, (b) 1 min, (c) 2 min, (d) 4 min and (e) 5 min.

Fig. 5(a) and (b) show morphological changes after calcination at 450 °C of the nanostructures shown in Fig. 1(c) and Fig. 3(c), respectively. The figures reveal that a portion of the structures disappears, thus indicating that the structures partially shrink. Similar to previous reports on the formation of ZnO,[15] the nanowires become nano-nodal structures after annealing. As shown in Fig. 6, TEM analysis clearly demonstrates that the smooth nanowire with an amorphous phase transforms to a bundle of nanoparticles with a polycrystalline phase after annealing (see diffraction patterns shown in the insets).

Fig. 7 presents the results of an FT-IR analysis of the grass-like structure (Fig. 1(c) and Fig. 5(a)) and the nanowires (Fig. 3(c) and Fig. 5(b)) before and after annealing. Peaks around 3400, 1600, 1350 and 1300 cm^{-1} can be attributed to $\nu_s(H_2O)$, $\nu_{as}(C{=}C)$, $\nu_s(C{-}O) + \nu(C{-}H)$, and $\nu_s(C{-}O) + \delta(O{-}C{=}O)$, respectively.[16] Spectra **A** and **C** in Fig. 7 exhibit the same peaks displayed in nickel oxalate powder.[17] Note that **A** and **C** of Fig. 7 show peaks at 600 and 800 cm^{-1}, which can be ascribed to $\nu_s(C{-}O) + \delta(O{-}C{=}O)$ (see Fig. S3 (ESI†) for an enlarged view of Fig. 7 in the range of 400–1000 cm^{-1}), whereas distinct peaks at 600 and 800 cm^{-1} do not appear for spectra **B** and **D** of Fig. 7. This means that unannealed structures of the grass-like structure and the nanowires show the same peaks, reflecting nickel oxalate structures. The peak at 490 cm^{-1} is assigned to Ni–O bonding in the nickel oxalate

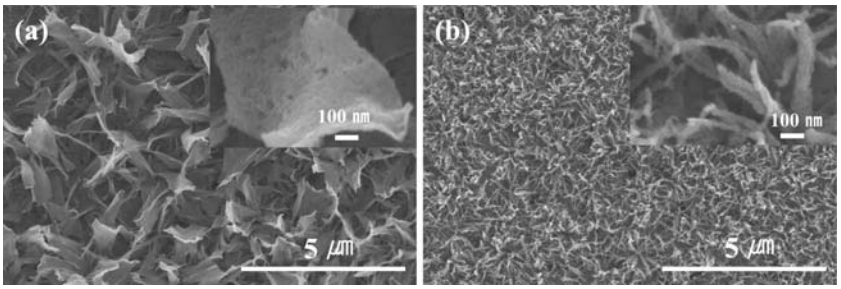

Fig. 5 Effects of annealing on the morphological changes of nanostructures: (a) after annealing of the grass-like morphology prepared in ethanolic 1 M oxalic acid without water addition, and (b) after annealing of nanowires prepared in ethanolic 1 M oxalic acid containing 5% water.

structure. The Ni–O peak shifts to a shorter wavelength when nanoparticles of nickel oxide are formed.[19] Thus, the sharp peak at 490 cm^{-1} for **C** in Fig. 7 (or Fig. S3(c), ESI†) can be ascribed to ν(Ni–O) bonding in the bulk phase nickel oxalate. On the other hand, the broad peak at 440 cm^{-1} shown for spectrum **D** of Fig. 7 (or Fig. S3(d), ESI†) can be attributed to Ni–O bonding in the nanostructured nickel oxide, which is confirmed by observation of the TEM image (Fig. 5(b)).[18,19] Therefore, we can conclude that the nickel oxalate nanowires can be converted into nickel oxide with a nanocrystalline phase after annealing.

Similar to previously reported results,[20] CV results for the four samples of Fig. 1(c), Fig. 3(c), Fig. 5(a) and Fig. 5(b) show double layer capacitances (Fig. 8(a)). As shown in **C** and **E** of Fig. 8(a), nickel oxide nanostructures show CV windows, implying double layer capacitance, which are larger than that of a thin NiO film prepared by annealing of a Ni foil at 450 °C for 120 min (**A** of Fig. 8(a)). Clearer windows are displayed in Fig. S3 (ESI†), which presents an enlarged view of Fig. 8. On the other hand, nickel oxalate structures show quasi-redox peaks (**B** and **D** of Fig. 8(a)). Thus, the CV scan ranges are extended from −0.25 to 0.4 V for pseudo-capacitance measurement. As shown in Fig. 8(b), the grass-like structure and nanowires display strong peaks at the redox potentials. Since this result was reproducibly obtained more than 50 times, we anticipate that the nickel oxide and nickel oxalate nanostructures can be exploited for

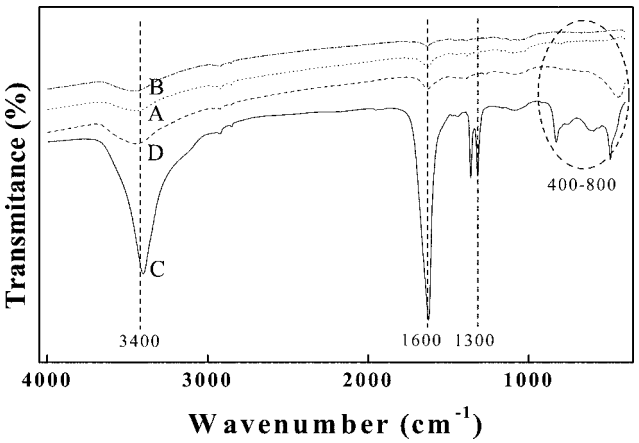

Fig. 7 FT-IR analysis of nanostructures. Spectrum **A** is of a grass-like structure before annealing (Fig. 1(c)); **B** is of a grass-like structure after annealing (Fig. 5(a)); **C** is of nanowires before annealing (Fig. 3(c)) and **D** is of nanowires after annealing (Fig. 5(b)). All structures are prepared in ethanolic 1 M oxalic acid with (or without) 5% water addition.

pseudo-capacitance. Interestingly, after annealing of the structures, the peaks are dramatically reduced, supporting that the nickel oxalate nanowires are better suited as supercapacitors. We suppose that nickel oxalate self-complex formation on the

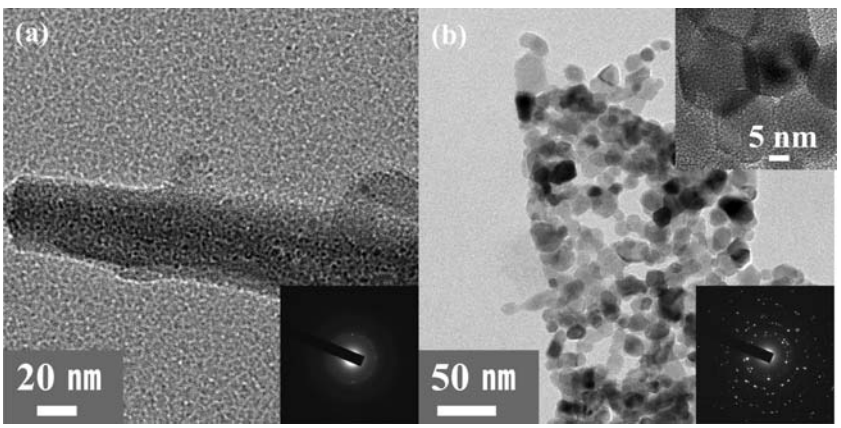

Fig. 6 TEM images of nanowires prepared in ethanolic 1 M oxalic acid containing 5% water for 1.5 h at 45 °C (a) before annealing, and (b) after annealing at 450 °C. The insets display diffraction patterns showing crystallinity.

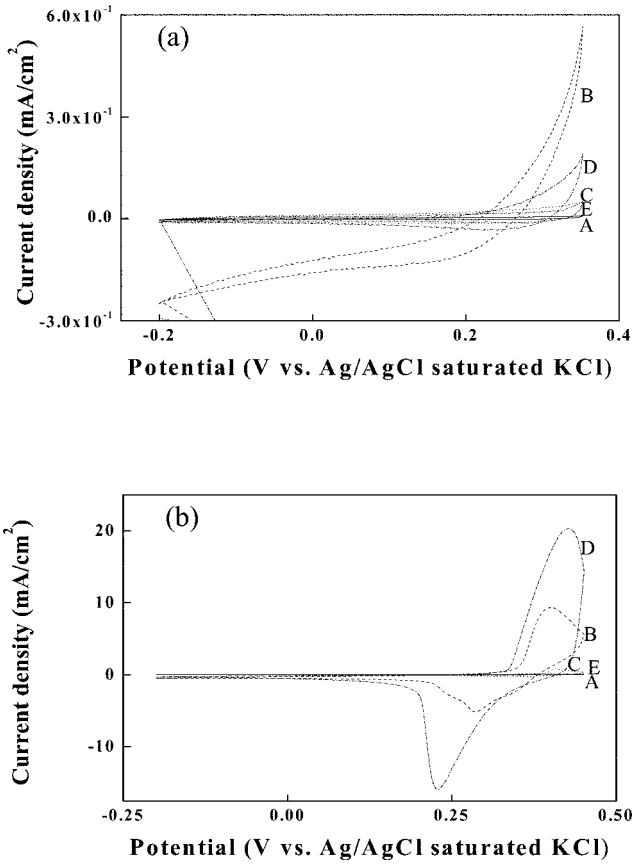

Fig. 8 Cyclic voltammograms of different samples in KOH at a scan rate of 25 mV s^{-1}: (a) scan range: −0.2 to 0.3, (b) scan range: −0.2 to 0.45. Note that **B**, **C**, **D** and **E** in (a) and (b) indicate the grass-like structure before annealing (Fig. 1(c)), the grass-like structure after annealing (Fig. 5(a)), the nanowires before annealing (Fig. 3(c)), and the nanowires after annealing (Fig. 5(b)), respectively. Voltammograms **A** in (a) and (b) are for nickel oxide on Ni foil, which is prepared by thermal annealing at 450 for 120 min.

surface of nickel oxalate nanowires in KOH is probably the origin of the redox mechanism of nickel as follows:[14]

$$2\ NiC_2O_4{\cdot}2H_2O\ (s) \leftrightarrow [Ni(C_2O_4)_2]^{2-}Ni^{2+}(aq)$$

Thus, the reduced and oxidized state of nickel (0 ↔ +2) can be cycled with electrochemical potential. More detailed investigation of why nickel oxalate structures show better performance compared to nickel oxide structures is currently underway.

3. Experimental

3.1. Preparation of solutions

First, 3.75 g of oxalic acid dihydrate ($C_2H_2O_4{\cdot}2H_2O$) corresponding to 1 M was dissolved into 100 ml of various solvents, *i.e.*, deionized water (>18 MΩ cm), methanol (≥99.8%), ethanol (≥99.9%), *n*-propanol (≥99.5%) and *n*-butanol (≥99.0%). Note that freshly prepared solutions should be used for the experiments. Otherwise, nanowires or grass-like structures cannot be produced by the method. For the fabrication of nanowires, a small amount of water was added into solutions containing oxalic acid.

3.2 Synthesis of NiC_2O_4, NiO and mixed-state nanowires

Ni foils with a thickness of 0.25 mm and a purity of 99.994% were purchased from Johnson Matthey Company. The Ni foils were cleaned with ethanol in an ultrasonic bath for 5 min. Subsequently, they were washed with deionized water and dried under a stream of N_2 gas. The cleaned nickel foil was immersed in the prepared solution. The reaction in the solution was then kept at 45 °C for 1.5 h without stirring. After the reaction was completed, the Ni foil was washed several times with deionized water and dried in a dry oven at 60 °C for 1 h.

3.3. Calcinations

For the synthesis of NiO nanowires, the as-prepared nanostructures were heated to 450 °C at a heating rate of 5 °C min^{-1} in air by using a muffle furnace and annealing of the nanostructures at 450 °C was carried out for 2 h.[21] This allowed the preparation of nanowires with a higher content of NiO.

3.4. Characterizations

The morphology of nanostructures prepared by the various methods was characterized using a field emission scanning electron microscope (FE-SEM, Hitachi, S-4300). Before FE-SEM measurements, the samples were first coated with a Pt layer by a sputter coater. Fourier-transform infrared spectroscopy (FT-IR, JASCO V-460) with a resolution of 2–4 cm^{-1} was employed to reveal the chemical composition of the nanostructures on the Ni foils. In addition, the composition and morphology of the nanostructures were characterized using a transmission electron microscope (TEM, Philips, CM200).

3.5. Electrochemical measurement for capacitance

Double layer capacitance and pseudo-capacitance of the nanostructures were characterized by cyclic voltammetry in a three-electrode cell with 1 M KOH electrolyte. The potential was cycled at scan rate of 25 mV s^{-1} in a range of 0.2 to 0.45 V using a potentiostat/galvanostat (AutoLab PGSTAT12, Eco Chemie) interfaced to a computer.

4. Conclusion

A method for the facile preparation of nickel oxalate and nickel oxide nanostructures has been described in detail. We demonstrated that a grass-like structure can be transformed to nanowires if a small amount of water is added. When the water content is increased, the diameter of the formed nickel oxalate nanowires becomes large, since the absolute amount of H^+ and OH^- increases; H^+ and OH^- promote dissolution of nickel, thus providing free nickel ions in solution. Self-complexes of nickel oxalate, which is the source for precipitation, are formed in a solution containing nickel ions and oxalate ions. As a result, directionally grown nanowires are prepared by preferential precipitation. The formed nickel oxalate structures can be

changed to nickel oxide structures after annealing. This is clearly supported by FT-IR and TEM measurements.

Supercapacitance of the nanostructures was investigated by cyclic voltammetry. We showed that the supercapacitance of the nickel oxalate structures is superior to that of the nickel oxide structures.

Acknowledgements

This work was financially supported by the Korean Ministry of Knowledge Economy through the New and Renewable Energy Center under contract number 2008-N-FC08-P-01.

References

1 B. E. Conway, in *Electrochemical Supercapacitors: Scientific Fundamentals and Technological Applications*, Kluwer Academic/Plenum Press, New York, 1999, (ch. 2), pp. 11–31.
2 M. Winter and R. J. Brodd, *Chem. Rev.*, 2004, **104**, 4245.
3 H. Y. Lee and J. B. Goodenough, *J. Solid State Chem.*, 1999, **144**, 220.
4 J. P. Zheng, P. J. Cygan and T. R. Zow, *J. Electrochem. Soc.*, 1995, **142**, 2699.
5 C. C. Hu and T. W. Tsou, *Electrochem. Commun.*, 2002, **4**, 105.
6 C. Lin, J. A. Ritter and B. N. Popov, *J. Electrochem. Soc.*, 1998, **145**, 4097.
7 P. A. Nelson and J. R. Owen, *J. Electrochem. Soc.*, 2003, **150**, A1313.
8 V. Ganesh and V. Lakshminarayanan, *Electrochim. Acta*, 2004, **49**, 3561.
9 K. W. Nam and K. B. Kim, *J. Electrochem. Soc.*, 2002, **149**, A346.
10 K. H. Chang, C. C. Hu and C. Y. Chou, *Chem. Mater.*, 2007, **19**, 2112.
11 C. Z. Yuan, L. Chen, B. Gao, L. H. Su and X. G. Zhang, *J. Mater. Chem.*, 2009, **19**, 246.
12 T. Nathan, A. Aziz, A. F. Noor and S. R. S. Prabaharan, *J. Solid State Electrochem.*, 2008, **12**, 1003.
13 C. Yuan, X. Zhang, L. Su, B. Gao and L. Shen, *J. Mater. Chem.*, 2009, **19**, 5772.
14 J. A. Allen, *J. Phys. Chem.*, 1953, **57**, 715.
15 S. J. Kim and J. Choi, *J. Cryst. Growth*, submitted.
16 G. J. Li, X. X. Huang, Y. Shi and J. K. Guo, *Mater. Lett.*, 2001, **51**, 325.
17 M. Salavati-Niasari, N. Mir and F. Davar, *Polyhedron*, 2009, **28**, 1111.
18 Y. Wang, J. Zhu, X. Yang, L. Lu and X. Wang, *Thermochim. Acta*, 2005, **437**, 106.
19 X. H. Huang, J. P. Tu, X. H. Xia, X. L. Wang and J. Y. Xiang, *Electrochem. Commun.*, 2008, **10**, 1288.
20 M. S. Wu, Y. A. Huang, J. J. Jow, W. D. Yang, C. Y. Hsieh and H. M. Tsai, *Int. J. Hydrogen Energy*, 2008, **33**, 2921.
21 X. Wang, J. Song, L. Gao, J. Jin, H. Zheng and Z. Zhang, *Nanotechnology*, 2005, **16**, 37.